Accuracy Studies for TDOA and TOA Localization

Regina Kaune
Dept. SDF
Fraunhofer FKIE/University of Bonn
Wachtberg, Germany
regina.kaune@fkie.fraunhofer.de

***Abstract*—In sensor networks, passive localization can be performed by exploiting the received signals of unknown emitters. In this paper, the Time of Arrival (TOA) measurements are investigated. Often, the unknown time of emission is eliminated by calculating the difference between two TOA measurements where Time Difference of Arrival (TDOA) measurements are obtained. In TOA processing, additionally, the unknown time of emission is to be estimated. Therefore, the target state is extended by the unknown time of emission. A comparison is performed investigating the attainable accuracies for localization based on TDOA and TOA measurements given by the Cramér-Rao Lower Bound (CRLB). Using the Maximum Likelihood estimator, some characteristic features of the cost functions are investigated indicating a better performance of the TOA approach. But counterintuitive, Monte Carlo simulations do not support this indication, but show the comparability of TDOA and TOA localization.**

Keywords: TOA, TDOA, CRLB, multilateration, sensor networks.

I. Introduction

Localization in sensor networks using passive measurements from an unknown emitter can be based on various types of measurements like Angle of Arrival (AOA), Time of Arrival (TOA), Frequency of Arrival (FOA) or Received Signal Strength (RSS). In this paper, the focus is on multilateration which is based on TOA or Time Difference of Arrival (TDOA) measurements of transmitted signals. Several distributed, time-synchronized sensors measure the TOA of a signal emitted by the unknown target. Often, the unknown time of emission is eliminated by calculating the difference between two TOA measurements where TDOA measurements are obtained. Usually, in a passive scenario, correlating the signals received at two different sensors delivers the TDOA measurements. Alternative, knowing some features of the signal, TOA measurements can be gained at a single sensor, [4], which can be processed to TDOA measurements.

TDOA localization is called hyperbolic positioning as illustrated in Fig. 1. A single noiseless TDOA measurement localizes the emitter on a hyperboloid or a hyperbola with the two sensors as foci. TOA measurements define spheres or circles as possible emitter positions (green circles in Fig. 1). For TOA localization, the parameter vector which is to be estimated is extended by the unknown time of emission.

TDOA and TOA localization has already been analyzed in many different aspects: an overview of hyperbolic positioning and passive localization is given in [10], [11]. Algorithms using a moving sensor pair are described in [6], [7], [8], [12].

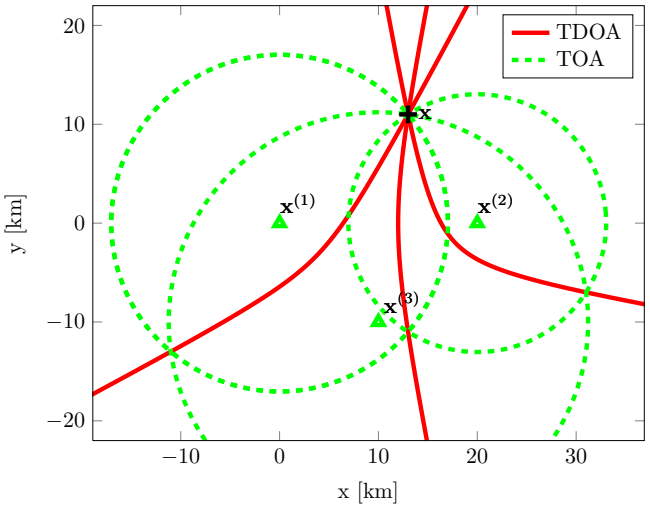

Fig. 1. Multilateration using TDOA and TOA measurements with hyperbolae and circles respectively as possible emitter locations

Closed form formulations in sensor networks can be found in [13] - [15]. An analysis of achievable localization accuracy is considered in [3], [16], [9].

In recent time, the focus of discussion is on direct use of TOA measurements without TDOA processing. Prerequisite for the direct TOA approach is the availability of TOA measurements: in active scenarios, it is no problem to determine the TOAs at a single sensor due to the knowledge on the emitted signal. In passive localization, there are different types of scenarios. Firstly, for non-cooperative scenarios, TOA measurements cannot be provided at a single sensor. The reason is, that signals need to be transmitted to a reference sensor or a fusion center to obtain TDOA measurements by cross correlation. Secondly, if there exists knowledge on the signal structure, like in cooperative or semi-cooperative passive scenarios, the TOA estimation at a single sensor is possible, see [4]. [1] investigates the error characteristics of TDOA and TOA localization for a cooperative scenario: the superior performance for the TOA compared to the TDOA processing is shown for localization of mobile nodes using a fixed reference sensor, a large sensor number and emitters in the inner area between sensors. [2] describes the TOA processing for a semi-cooperative scenario.

For gaining TDOA measurements, sensors must be paired.

There exist different TDOA measurement sets. Firstly, TDOA measurements can be received using a common reference sensor. Dependent on the choice of reference sensor, different measurement sets are obtained. In algorithms, often the case of a fixed reference sensor is assumed, for example [1]. Secondly, considering all possible sensor pairings yields the full measurement set with a larger number of measurements. In this paper, a comparison is performed using different reference sensors for a sensor network of three stationary sensors. The transfer to a larger network is analogue. The attainable accuracies for the full measurement set using all possible sensor pairs and measurement sets with fixed but different reference sensors are computed and analyzed.

The contribution of the paper is a comparison of the error bounds of localization for TDOA and TOA processing using the Cramér-Rao Lower Bound (CRLB). For a network of three sensors, the equality of the theoretical lower bound is shown for TOA and TODA localization with a fixed reference sensor. Additionally, the choice of reference sensor assuming constant variances for the measurements, does not impact the attainable accuracies. A Maximum Likelihood (ML) estimator is implemented to estimate the emitter state where the unknown time of emission is treated as nuisance parameter. Characteristic features of the cost functions give reason to expect a superior performance for TOA compared to TDOA localization. But Monte Carlo simulations show the equal estimation performance of TOA and TDOA localization.

The paper is organized as follows: in Section II, the principles of TOA and TDOA localization are outlined. Section III investigates the attainable accuracies in terms of the CRLB. The description of the estimation algorithm for TDOA and TOA processing follows in Section IV. Characteristic features of the cost functions are evaluated in Section V. Monte Carlo simulations analyze the performance of the two algorithms, Section VI. In Section VII, the main points of the paper are summarized.

II. Scenarios

An unknown stationary emitter $\mathbf{x} = (x, y)^T \in \mathbb{R}^2$ sends a signal which several time-synchronized stationary sensors $\mathbf{x}^{(i)}$, $i = 1, \dots M$, receive. A passive scenario is considered. Therefore, sensors do not send signals to illuminate the region of interest. They work passively and exploit the signal received from the emitter.

A. TOA scenario

At a single sensor, the TOA of the signal is determined. The TOA is composed of the emitting time t_0 and the time the signal needs to propagate the distance between emitter and sensor i:

$$\mathrm{TOA} = t_0 + \frac{r_i}{c}, \tag{1}$$

where

$$\begin{aligned} r_i &= ||\mathbf{x} - \mathbf{x}^{(i)}|| \\ &= \sqrt{(x - x^{(i)})^2 + (y - y^{(i)})^2}, \quad i = 1, \dots, M \end{aligned} \tag{2}$$

denotes the Euclidean distance between the emitter and sensor i and c is the speed of light.

By multiplication the TOA measurements in the time domain with the speed of light c the range measurement function is obtained:

$$h_i = r_0 + r_i, \tag{3}$$

where $r_0 = c\, t_0$ is the unknown time of emission multiplied with c.

Knowing or estimating the time of emission, a single TOA measurement localizes the emitter on a sphere, for two-dimensional localization on a circle. Fig. 1 shows a typical TOA scenario with three stationary sensors, green circles illustrate the geometrical interpretation of the TOA measurements.

In practice, TOA measurements are noisy. The TOA measurement noise is modeled as additive white Gaussian noise with standard deviation σ_i, for $i = 1, \dots, M$ and assumed to be uncorrelated from each other and from time step to time step:

$$z_i = h_i(\mathbf{x}) + v, \quad v \sim \mathcal{N}(0, \sigma_i^2). \tag{4}$$

Due to the Gaussian measurement noise, the Likelihood function $p(z_i|\mathbf{x})$ for a single TOA measurement is given by:

$$p(z_i|\mathbf{x}) = \frac{1}{\sqrt{2\pi}\sigma_i} \exp\left(-\frac{1}{2\sigma_i^2}(z_i - h_i(\mathbf{x}))^2\right). \tag{5}$$

The Likelihood function for the complete measurement set $\mathbf{z}_{\mathrm{t}} = (z_1, \dots, z_M)^T$ is expressed by:

$$\begin{aligned} &p(\mathbf{z}_{\mathrm{t}}|\mathbf{x}) = \\ &\frac{1}{\sqrt{|2\pi\mathbf{R}_{\mathrm{t}}|}} \exp\left(-\frac{1}{2}(\mathbf{z}_{\mathrm{t}} - \mathbf{h}_{\mathrm{t}}(\mathbf{x}))^T \mathbf{R}_{\mathrm{t}}^{-1}(\mathbf{z}_{\mathrm{t}} - \mathbf{h}_{\mathrm{t}}(\mathbf{x}))\right), \end{aligned} \tag{6}$$

where $|\cdot|$ indicates the determinant, $\mathbf{h}_{\mathrm{t}}(\mathbf{x}) = (h_1(\mathbf{x}), \dots, h_M(\mathbf{x}))^T$ is the measurement function and the covariance matrix is given by:

$$\mathbf{R}_{\mathrm{t}} = \begin{pmatrix} \sigma_1^2 & 0 & \dots & 0 \\ 0 & \sigma_2^2 & \ddots & \vdots \\ \vdots & \ddots & \ddots & 0 \\ 0 & \dots & 0 & \sigma_M^2 \end{pmatrix}. \tag{7}$$

B. TDOA scenario

TDOA measurements are obtained by calculating the difference between two TOA measurements and eliminating the unknown time of emission. Therefore, the sensors must be paired to get TDOA measurements. Multiplication with the speed of light c yields the measurement functions of range differences:

$$h_{ij} = r_i - r_j, \quad i, j \in \{1, \dots M\} \ \wedge j \neq i \tag{8}$$

Assuming additive white Gaussian noise uncorrelated from time step to time step and from each other, the measurement equations follow:

$$\begin{aligned} z_{ij} &= h_{ij}(\mathbf{x}_k) + v_{ij}, \\ &i, j \in \{1, \dots, M\} \ \wedge i \neq j, \quad v_{ij} \sim \mathcal{N}(0, \sigma_i^2 + \sigma_j^2) \end{aligned} \tag{9}$$

where the measurement noise $v_{ij} = v_i + v_j$ is composed of the noises at the two associated sensors and has the covariance $\sigma_i^2 + \sigma_j^2$.

For TDOA processing, different measurement sets are to be distinguish. Using a common reference sensor, M different measurement sets consisting of $M-1$ measurements can be obtained. The full measurement set contains $\sum_{l=1}^{M-1} l = \frac{M(M-1)}{2}$ measurements, here, all possibilities of sensor pairing are performed. Let sensor i be the reference sensor. Then, the measurements using a fixed reference sensor are defined by:

$$\begin{aligned} z_{ij} &= h_{ij}(\mathbf{x}_k) + v_{ij}, \\ & i,j \in \{1,\dots,M\} \ \wedge \ j \neq i, \end{aligned} \tag{10}$$

where i is fixed.

The measurements of the full measurement set are given by:

$$\begin{aligned} z_{ij} &= h_{ij}(\mathbf{x}_k) + v_{ij}, \\ & i = \{1,\dots M\}, j \in \{2,\dots,M\} \ \wedge \ j > i, \end{aligned} \tag{11}$$

where all sensor pairings are considered.

A single TDOA measurement defines a hyperboloid of possible target locations with the two sensors as foci. If sensors and emitter are located in the same plane, the emitter is located on a hyperbola. In Fig. 1, the green hyperbolic curves represent the full TDOA measurement set.

The measurement equation depends only on the emitter position, and the known positions of the sensors enter as parameters. Therefore, we have a two-dimensional localization problem. The two-dimensional position vector of the emitter is to be estimated.

In the following, a sensor network of three stationary sensors is considered. Let sensor 1 be the reference sensor. The Likelihood function for the measurement vector $\mathbf{z}_{\Delta t1} = (z_{12}, z_{13})^T$ and the measurement function $\mathbf{h}_{\Delta t1} = (h_{12}, h_{13})^T$ can be formulated as:

$$p(\mathbf{z}_{\Delta t1}|\mathbf{x}) = \frac{1}{\sqrt{|2\pi \mathbf{R}_{\Delta t1}|}} \exp\left(-\frac{1}{2}(\mathbf{z}_{\Delta t1} - \mathbf{h}_{\Delta t1}(\mathbf{x}))^T \mathbf{R}_{\Delta t1}^{-1} (\mathbf{z}_{\Delta t1} - \mathbf{h}_{\Delta t1}(\mathbf{x}))\right), \tag{12}$$

where $\mathbf{R}_{\Delta t1}$ is the covariance matrix of the measurement set. According to [3], the standard deviation can be dependent on the distances between emitter and sensors, but this distance dependency is here neglected. In this paper, the case of constant standard deviations with different values at single sensors is assumed:

$$\mathbf{R}_{\Delta t1} = \begin{pmatrix} \sigma_1^2 + \sigma_2^2 & \sigma_1^2 \\ \sigma_1^2 & \sigma_1^2 + \sigma_3^2 \end{pmatrix}. \tag{13}$$

Using sensor 2 as reference sensor, the covariance matrix has following form:

$$\mathbf{R}_{\Delta t2} = \begin{pmatrix} \sigma_2^2 + \sigma_1^2 & \sigma_2^2 \\ \sigma_2^2 & \sigma_2^2 + \sigma_3^2 \end{pmatrix}. \tag{14}$$

The covariance for the measurement vector using sensor 3 is:

$$\mathbf{R}_{\Delta t3} = \begin{pmatrix} \sigma_3^2 + \sigma_1^2 & \sigma_3^2 \\ \sigma_3^2 & \sigma_3^2 + \sigma_2^2 \end{pmatrix}. \tag{15}$$

For three sensors, the full measurement set $\mathbf{z}_{\Delta t\text{full}} = (z_{12}, z_{13}, z_{23})^T$ consists of three measurements. The associated covariance matrix is a 3×3 matrix:

$$\mathbf{R}_{\Delta t\text{full}} = \begin{pmatrix} \sigma_1^2 + \sigma_2^2 & \sigma_1^2 & \sigma_2^2 \\ \sigma_1^2 & \sigma_1^2 + \sigma_3^2 & \sigma_3^2 \\ \sigma_2^2 & \sigma_3^2 & \sigma_2^2 + \sigma_3^2 \end{pmatrix}. \tag{16}$$

III. CRLB ANALYSIS

The Cramér-Rao lower bound (CRLB) provides a lower bound on the covariance that is asymptotically achievable by any unbiased estimation algorithm based on the measurement vector $\mathbf{z}$, [5], [3]. It is calculated from the inverse of the Fisher Information Matrix (FIM) $\mathbf{J}$. Let the emitter location $\mathbf{x} \in \mathbb{R}^2$ be the parameter of interest and $\hat{\mathbf{x}}$ an estimate of it obtained from the measurement vector $\mathbf{z}$. Then the error covariance $\mathbb{E}\left[(\hat{\mathbf{x}} - \mathbf{x})(\hat{\mathbf{x}} - \mathbf{x})^T\right]$ is bounded below by:

$$\mathbb{E}\left[(\hat{\mathbf{x}} - \mathbf{x})(\hat{\mathbf{x}} - \mathbf{x})^T\right] \geq \mathbf{J}^{-1}, \tag{17}$$

$$\mathbf{J} = \mathbb{E}\left[\nabla_{\mathbf{x}} \ln p(\mathbf{z}|\mathbf{x}) (\nabla_{\mathbf{x}} \ln p(\mathbf{z}|\mathbf{x}))^T\right], \tag{18}$$

where $\mathbb{E}[\cdot]$ determines the expectation value.

A. TOA accuracy

In TOA processing, additionally the unknown time of emission t_0 is to be estimated. Therefore, for localization, the parameter of interest is the extended position state of the emitter:

$$\mathbf{x}^{(+)} = (t_0, \mathbf{x}^T)^T \in \mathbb{R}^3 \tag{19}$$

Given the measurement vector $\mathbf{z}_t$, the CRLB for TOA localization for one time step is computed from the inverse of the Fisher information for TOA, a 3×3 matrix:

$$\mathbf{J}_t = \frac{\partial \mathbf{h}_t^T}{\partial \mathbf{x}^{(+)}} \mathbf{R}_t^{-1} \frac{\partial \mathbf{h}_t}{\partial \mathbf{x}^{(+)}} \tag{20}$$

The Jacobian of the measurement function is:

$$\frac{\partial \mathbf{h}_t}{\partial \mathbf{x}^{(+)}} = \begin{pmatrix} \frac{\partial h_1}{\partial t_0} & \frac{\partial h_1}{\partial x} & \frac{\partial h_1}{\partial y} \\ \frac{\partial h_2}{\partial t_0} & \frac{\partial h_2}{\partial x} & \frac{\partial h_1}{\partial y} \\ \frac{\partial h_3}{\partial t_0} & \frac{\partial h_3}{\partial x} & \frac{\partial h_1}{\partial y} \end{pmatrix} = \begin{pmatrix} c & \frac{x-x_1}{r_1} & \frac{y-y_1}{r_1} \\ c & \frac{x-x_2}{r_2} & \frac{y-y_2}{r_2} \\ c & \frac{x-x_3}{r_3} & \frac{y-y_3}{r_3} \end{pmatrix}. \tag{21}$$

The computation of the FIM follows as:

$$\begin{aligned} \mathbf{J}_t &= \begin{pmatrix} c & c & c \\ \frac{x-x_1}{r_1} & \frac{x-x_2}{r_2} & \frac{x-x_3}{r_3} \\ \frac{y-y_1}{r_1} & \frac{y-y_2}{r_2} & \frac{y-y_3}{r_3} \end{pmatrix} \begin{pmatrix} \frac{1}{\sigma_1^2} & 0 & 0 \\ 0 & \frac{1}{\sigma_2^2} & 0 \\ 0 & 0 & \frac{1}{\sigma_3^2} \end{pmatrix} \begin{pmatrix} c & \frac{x-x_1}{r_1} & \frac{y-y_1}{r_1} \\ c & \frac{x-x_2}{r_2} & \frac{y-y_2}{r_2} \\ c & \frac{x-x_3}{r_3} & \frac{y-y_3}{r_3} \end{pmatrix} \\ &= \sum_{i=1}^{3} \begin{pmatrix} \frac{c^2}{\sigma_i^2} & \frac{c}{\sigma_i^2}\frac{x-x_i}{r_i} & \frac{c}{\sigma_i^2}\frac{y-y_i}{r_i} \\ \frac{c}{\sigma_i^2}\frac{x-x_i}{r_i} & \frac{1}{\sigma_i^2}\frac{(x-x_i)^2}{r_i^2} & \frac{1}{\sigma_i^2}\frac{(x-x_i)(y-y_i)}{r_i^2} \\ \frac{c}{\sigma_i^2}\frac{y-y_i}{r_i} & \frac{1}{\sigma_i^2}\frac{(x-x_i)(y-y_i)}{r_i^2} & \frac{1}{\sigma_i^2}\frac{(y-y_i)^2}{r_i^2} \end{pmatrix}. \end{aligned} \tag{22}$$

The Fisher information can be expressed by:

$$\mathbf{J}_{\mathrm{t}} = \begin{pmatrix} J_{11} & J_{12} & J_{13} \\ J_{21} & J_{22} & J_{23} \\ J_{31} & J_{32} & J_{33} \end{pmatrix} = \begin{pmatrix} J_{\mathrm{t}} & J_{\mathrm{t,pos}} \\ J_{\mathrm{pos,t}} & \mathbf{J}_{\mathrm{pos}} \end{pmatrix}, \tag{23}$$

where $\mathbf{J}_{pos}$ is the Fisher information of the position space, J_t The FIM of the time space and the others are the cross terms. According to [1], the CRLB of the position space can be computed using the matrix inversion lemma. The time of emission is treated as nuisance parameter. The resulting CRLB for the position space is the same as for TDOA localization.

It can be shown that $\mathbf{J}_{\mathrm{pos}} = \mathbf{J}_{\Delta \mathrm{ti}}$, $i = 1, \ldots, 3$.

B. TDOA accuracy

For TDOA localization, different measurement sets are to be considered: the full measurement set and measurement sets using a fixed reference sensor.

Analogue to (20), the FIM for TDOA localization (one time step) is given by (this equation can be applied to all different measurements sets using the appropriate indices):

$$\mathbf{J}_{\Delta \mathrm{t}} = \frac{\partial \mathbf{h}_{\Delta \mathrm{t}}}{\partial \mathbf{x}} \mathbf{R}_{\Delta \mathrm{t}}^{-1} \frac{\partial \mathbf{h}_{\Delta \mathrm{t}}}{\partial \mathbf{x}} \tag{24}$$

The Jacobian of the measurement set with sensor 1 as reference sensor is:

$$\begin{aligned} \frac{\partial \mathbf{h}_{\Delta \mathrm{t1}}}{\partial \mathbf{x}} &= \begin{pmatrix} \frac{\partial r_{12}}{\partial x} & \frac{\partial r_{12}}{\partial y} \\ \frac{\partial r_{13}}{\partial x} & \frac{\partial r_{13}}{\partial y} \end{pmatrix} \\ &= \begin{pmatrix} \frac{x-x_1}{r_1} - \frac{x-x_2}{r_2} & \frac{y-y_1}{r_1} - \frac{y-y_2}{r_2} \\ \frac{x-x_1}{r_1} - \frac{x-x_3}{r_3} & \frac{y-y_1}{r_1} - \frac{y-y_3}{r_3} \end{pmatrix}, \end{aligned} \tag{25}$$

The FIM is computed as:

$$\mathbf{J}_{\Delta \mathrm{t1}} = \begin{pmatrix} F_{11} & F_{12} \\ F_{21} & F_{22} \end{pmatrix}, \tag{26}$$

$$\begin{aligned} F_{11} &= \frac{1}{l} \sum_{i=1}^{3} \sum_{j \neq i} \sigma_j^2 \frac{(x-x_i)^2}{r_i} \\ &\quad - \frac{1}{l} \sum_{i=1}^{2} \sum_{j=i+1}^{3} \sum_{k \neq i,j} 2\sigma_k^2 \frac{(x-x_i)(x-x_j)}{r_i r_j} \end{aligned} \tag{27}$$

$$\begin{aligned} F_{22} &= \frac{1}{l} \sum_{i=1}^{3} \sum_{j \neq i} \sigma_j^2 \frac{(y-y_i)^2}{r_i} \\ &\quad - \frac{1}{l} \sum_{i=1}^{2} \sum_{j=i+1}^{3} \sum_{k \neq i,j} 2\sigma_k^2 \frac{(y-y_i)(y-y_j)}{r_i r_j} \end{aligned} \tag{28}$$

$$F_{12} = F_{21} \tag{29}$$

$$\begin{aligned} &= \frac{1}{l} \sum_{i=1}^{3} \sum_{j \neq i} \sigma_j^2 \frac{(x-x_i)(y-y_i)}{r_i} \\ &\quad - \frac{1}{l} \sum_{i=1}^{3} \sum_{j \neq i} \sum_{k \neq i,j} \sigma_k^2 \frac{(x-x_i)(y-y_j)}{r_i r_j} \end{aligned} \tag{30}$$

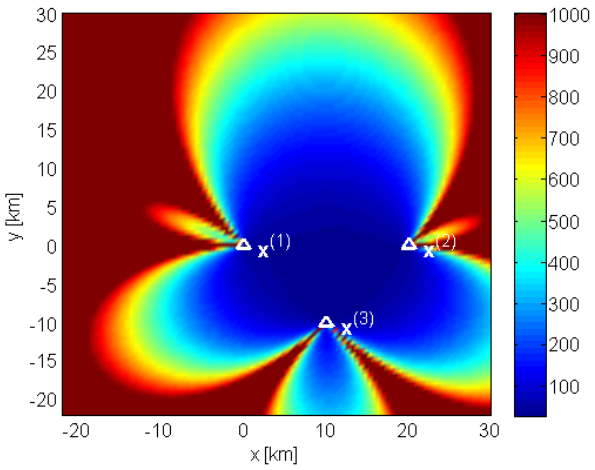

Fig. 2. CRLB plot for TDOA and TOA localization respectively

with

$$l = \sum_{i=1}^{2} \sum_{j=i+1}^{3} \sigma_i^2 \sigma_j^2. \tag{31}$$

This FIM is obtained for all measurement sets using a fixed but different reference sensor. Therefore, the choice of reference sensor does not influence the theoretical lower bound for the variance of an unbiased estimator. Using different reference sensors yields the same CRLB. Fig. 2 shows the CRLB for the scenario of Section VI using a network of three sensors. For a grid of possible emitter positions in the plane, the associated CRLB matrix (for TDOA = TOA) is computed. The square root of the trace is shown. For better visibility, values larger than 1000 m have been cut off. The color bar gives the CRLB values. Sensor positions are marked with white triangles.

The Jacobian of the measurement function vector of the full measurement set is:

$$\frac{\partial \mathbf{h}_{\Delta \mathrm{tfull}}^T}{\partial \mathbf{x}} = \begin{pmatrix} \frac{\partial h_{12}}{\partial x} & \frac{\partial h_{12}}{\partial y} \\ \frac{\partial h_{13}}{\partial x} & \frac{\partial h_{13}}{\partial y} \\ \frac{\partial h_{23}}{\partial x} & \frac{\partial h_{23}}{\partial y} \end{pmatrix} \tag{32}$$

$$= \begin{pmatrix} \frac{x-x_1}{r_1} - \frac{x-x_2}{r_2} & \frac{y-y_1}{r_1} - \frac{y-y_2}{r_2} \\ \frac{x-x_1}{r_1} - \frac{x-x_3}{r_3} & \frac{y-y_1}{r_1} - \frac{y-y_3}{r_3} \\ \frac{x-x_2}{r_2} - \frac{x-x_3}{r_3} & \frac{y-y_2}{r_2} - \frac{y-y_3}{r_3} \end{pmatrix}. \tag{33}$$

The computation of the FIM for the full measurement set gives different entries as for the measurement set with a fixed reference sensor. There is an information gain in processing the full TDOA set indicating a smaller theoretical lower bound. The diagonal entries of the FIM of the full TDOA

measurement set are given by:

$$
\begin{aligned}
F_{11}^{\text{full}} &= \frac{1}{l}\sum_{i=1}^{3}\sum_{j\neq i}\sigma_j^2\frac{(x-x_i)^2}{r_i} + \frac{2}{l}\sigma_2^2\frac{(x-x_2)^2}{r_2} \\
&+ \frac{1}{l}\sum_{i\neq 2}^{3}\sum_{j\neq i}\left(\frac{\sigma_2^2\sigma_j^2}{\sigma_i^2}\frac{(x-x_i)^2}{r_i} + \frac{\sigma_2^2\sigma_j^2}{\sigma_i^2}\frac{(x-x_2)^2}{r_2}\right) \\
&- \frac{1}{l}\sum_{i\neq 2}\sum_{j\neq i}2(\sigma_2^2+\sigma_j^2)\frac{(x-x_2)(x-x_i)}{r_2 r_i} \\
&- \frac{1}{l}\sum_{i\neq 2}^{3}\sum_{j\neq i}\frac{\sigma_2^2\sigma_j^2}{\sigma_i^2}\frac{(x_2-x_i)^2}{r_2 r_i} \qquad (34)
\end{aligned}
$$

$$
\begin{aligned}
F_{22}^{\text{full}} &= \frac{1}{l}\sum_{i=1}^{3}\sum_{j\neq i}\sigma_j^2\frac{(y-y_i)^2}{r_i} + \frac{2}{l}\sigma_2^2\frac{(y-y_2)^2}{r_2} \\
&+ \frac{1}{l}\sum_{i\neq 2}^{3}\sum_{j\neq i}\left(\frac{\sigma_2^2\sigma_j^2}{\sigma_i^2}\frac{(y-y_i)^2}{r_i} + \frac{\sigma_2^2\sigma_j^2}{\sigma_i^2}\frac{(y-y_2)^2}{r_2}\right) \\
&- \frac{1}{l}\sum_{i\neq 2}\sum_{j\neq i}2(\sigma_2^2+\sigma_j^2)\frac{(y-y_2)(y-y_i)}{r_2 r_i} \\
&- \frac{1}{l}\sum_{i\neq 2}^{3}\sum_{j\neq i}\frac{\sigma_2^2\sigma_j^2}{\sigma_i^2}\frac{(y_2-y_i)^2}{r_2 r_i}. \qquad (35)
\end{aligned}
$$

Analyzing the diagonal entries of the FIM of the full measurement set, the main difference to the FIM using a fixed reference sensor are 6 additional positive terms and 6 additional negative terms (double terms are taken into account twice). The impact on the CRLB is dependent on the geometry and the values for the standard deviations and leads to different CRLBs for the full TDOA measurement set and the measurement set using a fixed reference sensor.

IV. Estimation algorithm

Due to the nonlinear measurement equations, nonlinear estimation methods are needed to solve the localization problem. There are several nonlinear methods like the Maximum Likelihood (ML) estimator, nonlinear forms of the Kalman Filter, like the Extended and the Unscented KF or for TDOA localization using a sufficient number of sensors, closed form formulations.

For TOA localization, an extended parameter vector is to use. For the purpose of comparing the TOA and TDOA results, the extended dimension, the time of emission, is treated as nuisance parameter. The MLE offers a good comparable solution for the TOA and the TDOA measurement sets.

A. TOA Localization

In TOA processing, additionally the unknown time of emission t_0 is to be estimated. The target state is extended by the unknown time of emission. Therefore, the extended position vector $\mathbf{x}^{(+)}$, see (19), is to be estimated.

The ML estimate is that value of the extended position vector $\mathbf{x}^{(+)}$ which maximizes the likelihood function or rather minimizes:

$$
\hat{\mathbf{x}}^{(+)} = \arg\min_{\mathbf{x}^+}\sum_{i=1}^{3}\frac{(z_i-h_i)^2}{\sigma_i^2} \qquad (36)
$$

It is realized with the simplex method due to Nelder and Mead as numerical iterative search algorithm. The two-dimensional initialization point is extended by the time of emission according to:

$$
t_0 = \frac{z_1}{c} - \frac{||\mathbf{x}_{\text{init}} - \mathbf{x}^{(1)}||}{c}. \qquad (37)
$$

B. TDOA Localization

For TDOA localization, the full measurement set and the measurement set using a fixed reference sensor are processed in a ML estimator (using the appropriate indices, the equation can be applied to all TDOA measurement sets):

$$
\hat{\mathbf{x}} = \arg\min_{\mathbf{x}}(\mathbf{z}_{\Delta t} - \mathbf{h}_{\Delta t}(\mathbf{x}))^T\mathbf{R}_{\Delta t}^{-1}(\mathbf{z}_{\Delta t} - \mathbf{h}_{\Delta t}(\mathbf{x})). \qquad (38)
$$

As in TOA localization, the same numerical iterative search algorithm is applied. The initialization point of the ML estimator is generated randomly from a Gaussian distribution centered at the true emitter position with standard deviation of 500 m in x and y direction.

V. Angles of intersection

While the CRLB describe the theoretical lower bound for localization, here, some practical aspects are taken into consideration. Using a nonlinear estimation method like the MLE, the global maximum of the cost function must be found. Therefore, the characteristics of the cost function are essential. The shape of the error ellipses depend on the value of the intersection angles of the emitter lines. In two-dimensional TOA localization, emitter lines are circles around the sensor positions. In TDOA localization, emitter lines are hyperbolae with the sensor positions as foci. The magnitude of the angles between two curves may influence the performance of the ML estimator. Intersecting circles and hyperbolae, the angles of intersection can be computed using the tangents in the intersection points.

A. TOA angles

The determination of the angles between the TOA circles can be performed in two steps:

- Computation of lines between the centers of the circles, that is the sensor positions, and the intersection points of circles.
- Intersection of lines and calculation of the angles of intersection; angles must be in the interval $[0, \frac{\pi}{2}]$ in radians or $[0°, 90°]$ in degrees. An angle near $0°$ means poor performance, an angle of $90°$ implies the best information gain and good performance. If the angle is in the interval $[90°, 180°]$, the opposite angle is calculated.

Fig. 3(a) shows angles of intersection plotted in the plane for a network of three sensors. For a grid of possible emitter positions in the plane, the angles of intersecting circles are

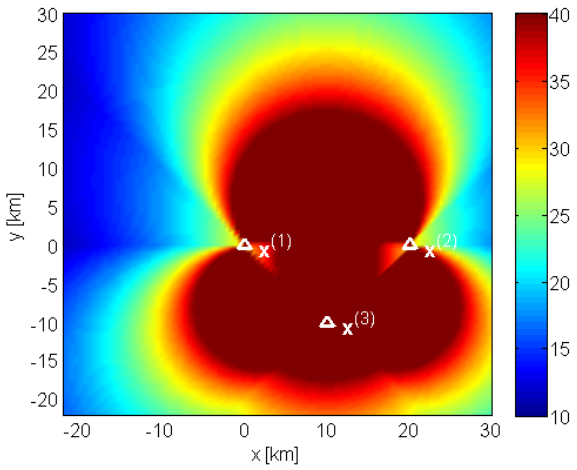

(a) TOA

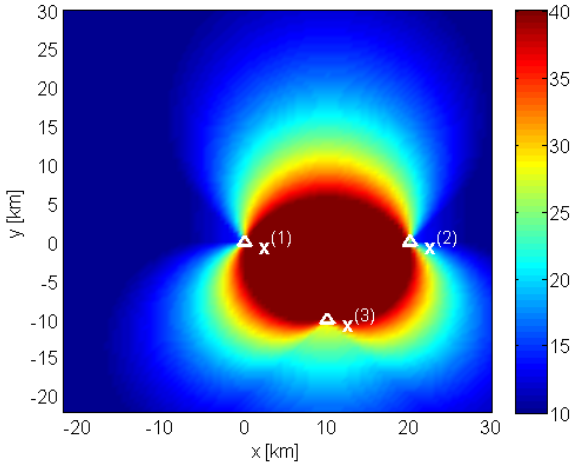

(b) TDOA

Fig. 3. Mean values of angles of intersection between circles and hyperbolae respectively

computed. For each grid point, the mean value of the three associated angles is plotted in the plane. Sensor positions are assumed as in the first scenario of Section VI and marked with white triangles. The color bar gives the values of mean angles in degree. For visualization purpose, values of angles have been cut off to $60°$. In the inner area, between sensor positions, the mean values of angles are high. Compared to TDOA, there exist a large region of large angles.

B. TDOA angles

The algorithm of determining angles between two TDOA hyperbolae is as follows:

- Computation of tangents at intersection points of two TDOA hyperbolae.
- Intersection of tangents and calculation of the angles of intersection; angles must be in the interval $[0, \frac{\pi}{2}]$ in radians or $[0°, 90°]$ in degrees, see above.

Angles of intersection in the plane are illustrated in Fig. 3(b). Results are computed using the full measurement set with 3 measurements. The field of large angles is much more limited than for TOA.

The results of the study on the angular size let expect a superior performance of the TOA localization compared to the TDOA localization. The superiority of the TOA processing is described in [1] for a large network of twelve sensors. In [1], the TDOA measurement set is gained using a fixed reference sensor, emitters are only in the inner area between sensors and localization of mobile emitters is performed. The present paper analyzes two different scenarios in Section VI. For TDOA, not only the measurement set using a fixed reference sensor is investigated, but also the full measurement set. Counterintuitive to the results of the angle study, in simulations, TDOA and TOA localization show almost equal localization performance.

VI. Simulation results

Two different localization scenarios are analyzed. For both scenarios, a grid of stationary emitter locations in the plane is investigated. In the first scenario, emitter localization is performed for a small sensor network of three stationary sensors. A large number of the analyzed emitters lies outside the inner area of the sensors where the expected localization accuracy is low. The second scenario analyzes a large network consisting of eight sensors. The inner area between the emitters covers most of the observation area.

Measurements are obtained using the stationary sensor network. TOA measurements are generated by adding white Gaussian noise with a standard deviation of 15 m in the range domain (50 nsec in the time domain) to the true values. Standard deviations of different sensors are assumed to be equal. TDOA measurements are obtained by calculating the difference between two TOA measurements. In this way, TOA and TDOA measurements underlie the same noise conditions and localization results are comparable.

The Root Mean Square Error (RMSE), the squared distance of the estimate to the true target location $\mathbf{x}$ is computed as performance measure. It is averaged over N, the number of Monte Carlo runs. Let $\hat{\mathbf{x}}(k)$ be the estimate of the kth run. Then, the RMSE at is computed as:

$$\text{RMSE} = \sqrt{\frac{1}{N}\sum_{k=1}^{N}(\mathbf{x}-\hat{\mathbf{x}}(k))^T(\mathbf{x}-\hat{\mathbf{x}}(k))}. \qquad (39)$$

For each grid point, 100 independent Monte Carlo runs are computed.

Fig. 4 illustrates the results for the sensor network using three sensors. Localization results are similar to the results of the CRLB analysis, see Fig. 2. Values for RMSE are cut off to 1000 m. The colorbar gives the localization results in m. White triangles designates the sensor positions. For TDOA localization, the full measurement set is used, the results for the measurement set with fixed reference sensor show only little differences, as well as the comparison of TDOA and TOA processing.

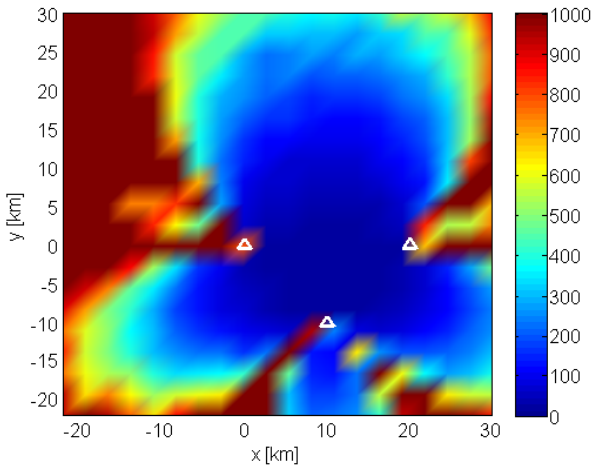

(a) TDOA using the full measurement set

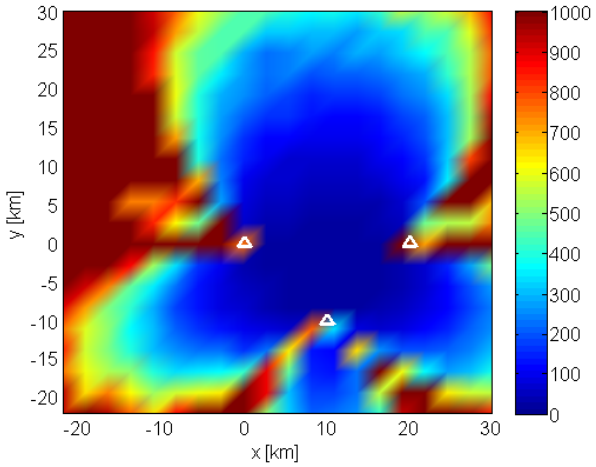

(b) TOA

Fig. 4. TDOA and TOA localization results

For the sake of simplicity, the ML estimator for the larger network is implemented as least squares algorithm where the covariance matrix of the measurement set is neglected. The localization results for the large sensor network consisting of 8 sensors are presented in Fig. 5. Most of the observation area lies in the inner region between sensor positions where the expected localization accuracy is high. The differences between TDOA and TOA localization are not significant. TDOA localization based on the full measurement set shows in the inner area between sensors better performance than the localization using a fixed reference sensor. Overall, TDOA and TOA localization yield roughly the same results.

These results do not support the expectations resulting from the angle study. One reason for the surprising performances is the larger dimensionality of the parameter vector for the TOA optimization process. The TOA cost function is minimized over three dimensions, but the angle study only investigates the projection in the position space. Analyzing the process of

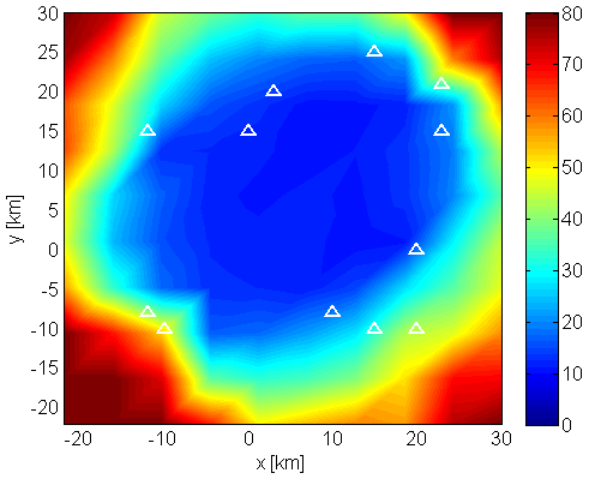

(a) TDOA using the full measurement set

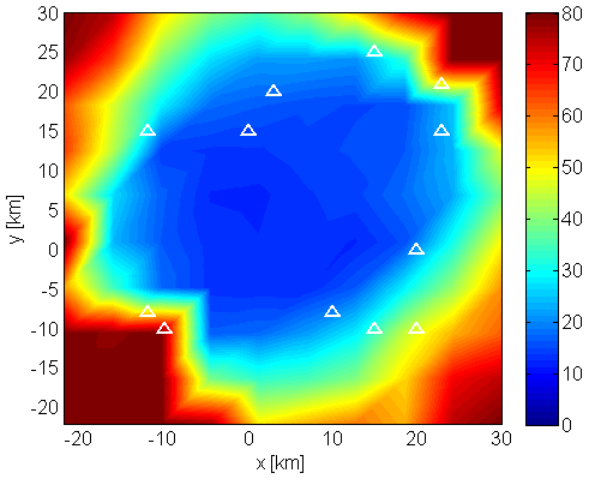

(b) TDOA using a fixed reference sensor

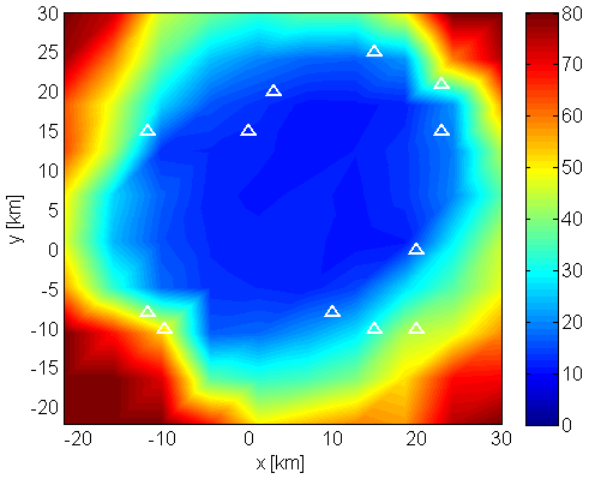

(c) TOA

Fig. 5. TDOA and TOA localization results using eight sensors

optimization, the number of iterations for TOA processing is larger than for TDOA processing. This indicates a larger sensitivity of the TOA optimization to the initialization point. For future research, it will be interesting to investigate additional reasons for the equal performance of TDOA and TOA. The fusion of TDOA and TOA and scenarios with known time of emission might be the topic of further analysis.

VII. Conclusions

In this paper, accuracy studies for TDOA and TOA localization are performed. For a network of three sensors, the CRLB are computed using the TDOA and the TOA measurement set. The theoretical lower bounds are identical for TOA localization and for TDOA localization using a fixed reference sensor. Additionally, the choice of reference sensor does not influence the CRLB. Assuming constant variance with different values at various sensors, the equality of the CRLB for different reference sensors is shown. Using the full TDOA measurement set, more information is processed for localization. The theoretical lower bounds are smaller than for TDOA localization with a fixed reference sensor.

While the theoretical bounds show no difference in TOA and TDOA localization with a fixed reference sensor, in practice, considerations like characteristics of the cost function must be taken into account. A study on the angles between two emitter lines may indicate difficulties of finding the maximum of cost function in TDOA processing. But counterintuitive, simulations do not support the superiority of the TOA localization but show almost equal performance of TOA compared to TDOA localization.

References

[1] T. Sathyan, M. Hedley and M. Mallick, *An analysis of the Error Characteristics of Two Time of Arrival Localization Techniques*, 13th International Conference on Information Fusion, Edinburgh, July 2010.

[2] A. Mathias, M. Leonardi and G. Galati, *An Efficient Multilateration Algorithm*, Proceedings of ESAV'08, Capri, Italy, Sept. 2008.

[3] R. Kaune, J. Hörst and W. Koch, *Accuracy Analysis for TDOA Localization in Sensor Networks*, 14th Int. Conf. on Information Fusion, Chicago (IL), USA, July 2011.

[4] C. Steffes, R. Kaune and S. Rau, *Determining Times of Arrival of Transponder Signals in a Sensor Network using GPS Time Synchronization*, Informatik 2011, Workshop Sensor Data Fusion: Trends, Solutions, Applications, Berlin, Germany, Oct. 2011.

[5] Y. Bar-Shalom, X. Rong Li, and T. Kirubarajan, *Estimation with Applications to Tracking and Navigation*, Wiley-Interscience, 2001.

[6] F. Fletcher, B. Ristic and D. Musicki, *Recursive Estimation of Emitter Location using TDOA Measurements from Two UAVs*, 10th Int. Conference on Information Fusion, Quebec, Canada, July 2007.

[7] R. Kaune, *Gaussian Mixture (GM) Passive Localization using Time Difference of Arrival (TDOA)*, Informatik 2009-Workshop Sensor Data Fusion: Trends, Solutions, Applications, 2009.

[8] R. Kaune, *Performance analysis of passive emitter tracking using TDOA, AOA and FDOA measurements*, Informatik 2010, Workshop Sensor Data Fusion: Trends, Solutions, Applications, Leipzig, Germany, Sept./Oct. 2010.

[9] T. Jia and R. M. Buehrer, *A New Cramer-Rao Lower Bound for TOA-based Localization*, Proceedings of IEEE MilCom 2008, Nov. 2008.

[10] D. J. Torrieri, *Statistical Theory of Passive Location Systems*, IEEE Trans. on Aerospace and Electronic Systems, 20(2): 183–198, March 1984.

[11] R. Kaune, D. Mušicki, W. Koch, *On passive emitter tracking*, chapter in Sensor Fusion and its Applications, edited by C. Thomas, publisher: sciyo, ISBN 978-953-307-101-5, pp. 293-318, www.intechweb.org, August 2010.

[12] D. Mušicki, R. Kaune, W. Koch, *Mobile Emitter Geolocation and Tracking Using TDOA and FDOA Measurements*, IEEE Trans. on Signal Processing, 58(3), part 2: 1863–1874, 2010.

[13] J. O. Smith and J. S. Abel, *Closed-Form Least-Squares Source Location Estimation from Range-Difference Measurements*, IEEE Trans. on Acoustics, Speech, and Signal Processing, ASSP-35(12):1661–1669, Dec. 1987.

[14] H. C. So, Y. T. Chan and F. K. W. Chan, *Closed-Form Formulae for Time-Difference-of-Arrival Estimation*, IEEE Trans. on Signal Processing, 56(6): 2614–2620, 2008.

[15] M. D. Gillette and H. F. Silverman, *A Linear Closed-Form Algorithm for Source Localization From Time-Differences of Arrival*, IEEE Signal Processing Letters, 15: 1–4, 2008.

[16] X. Hu and M. L. Fowler, *Sensor selection for multiple sensor emitter location systems*, IEEE Aerospace Conference '08, Big Sky, Nevada, March 2008.